Lysosome Lipid Storage Disorder in NCTR-BALB/c Mice

II. Morphologic and Cytochemical Studies

HELEN SHIO, MA, STANLEY FOWLER, PhD, CHIDAMBARAM BHUVANESWARAN, PhD, and MANFORD D. MORRIS, PhD

From the Laboratory of Biochemical Cytology, The Rockefeller University, New York, New York, and Departments of Biochemistry and Pediatrics, University of Arkansas for Medical Sciences, Little Rock, Arkansas

Electron-microscopic and cytochemical studies were carried out on tissues of NCTR-BALB/c mice. These mice are affected with a neurovisceral genetic disorder involving excessive tissue accumulation of lipid. Distinctive polymorphic intracellular inclusions, bounded by a membrane and containing lamellated bodies, were found in many cells of liver, spleen, lung, kidney, intestine, lymph nodes, and brain. The inclusions transformed reticuloendothelial cells into massive foam cells. Acid phosphatase cytochemical studies performed on sections of liver demonstrated that the inclusions were lysosomes. Fixation of liver in the presence of digitonin produced "spicules" in the inclusions characteristic of digitonin-cholesterol complexes. Clefts of cholesterol crystals were seen in the inclusions in liver, spleen, and lung. We conclude that the NCTR-BALB/c mice are affected by a lysosome lipid storage disease and that cholesterol is a major storage product. (Am J Pathol 1982, 108:150–159)

THE NEUROVISCERAL DISORDER affecting the NCTR strain of BALB/c mice was found to be associated with relative organ enlargement, extensive deposition of lipid, and appearance of vacuolated cells in many tissues.[1] Especially notable was the accumulation of large foam cells in reticuloendothelial system (RES)-rich tissues of affected mice. These pathologic features are characteristic of those of many inborn lysosomal storage diseases[2] and raise the possibility that the NCTR-BALB/c mice may be affected by such a condition. In this article we describe results of ultrastructural and cytochemical studies that support this conclusion and show that cholesterol is a major storage product. A preliminary communication of these investigations has been published previously.[3]

Supported by research grants HL-18157 and AM-21376 from the National Institutes of Health and PCM-8008713 from the National Science Foundation. Dr. Fowler conducted these studies during the tenure of an Otto G. Storm Established Investigatorship from the American Heart Association.

Accepted for publication March 10, 1982.

Dr. Fowler's present address is Department of Pathology, School of Medicine, University of South Carolina, Columbia, SC 29208.

Address reprint requests to Dr. Manford D. Morris, Department of Pediatrics, University of Arkansas for Medical Sciences, 4301 W. Markham, Little Rock, AR 72205.

0002-9440/82/0810-0150$01.30

Materials and Methods

Animals and Samples

Control BALB/c and affected NCTR-BALB/c mice, both male and female, aged 67–78 days were used in these studies. The affected NCTR-BALB/c mice exhibited the symptoms of the disorder described in the preceding article, and they were in the descending limb of their growth profile.[1] The mice were fed *ad libitum* on Purina Mouse Chow. Because of the progressive impairment of their coordination, the affected mice were less able to feed themselves and may have been semifasted at the time of sacrifice.

The mice were killed by cervical dislocation, and the brain, intestine, kidney, liver, lungs, lymph nodes (affected mice only) and spleen were immediately excised and fixed by immersion for morphologic study.

Electron Microscopy

Specimens of each tissue, diced into 1 cu mm pieces, were fixed 1–2 hours in ice-cold 2.5% glutaraldehyde (Electron Microscopy Sciences, Fort Washington, Pa) in 100 mM sodium cacodylate buffer, pH 7.4, or in paraformaldehyde–glutaraldehyde fixative[4] in the same cacodylate buffer. The samples were then postfixed for 1.5 hours in 1% osmium tetroxide in cacodylate buffer and stained *en bloc* with uranyl acetate.[5] After dehydration in graded alcohol and propylene oxide, the samples were embedded in Epon 812. Silver sections were cut on a Sorvall MT-2B ultramicrotome with a duPont diamond knife. They were doubly stained with uranyl acetate[6] and lead citrate.[7] Microscopy was performed with a Philips EM-300 electron microscope operated at 80 kv.

Cytochemistry

Acid Phosphatase

Cytochemical identification of lysosomes was made by acid phosphatase staining. Tissue specimens (approximately 1 × 2 × 10 mm) were fixed in 1–2% glutaraldehyde in 100 mM sodium cacodylate buffer, pH 7.4, for 1–2.5 hours on ice, and 30–40-μ thick sections were then chopped on a Smith-Farquhar TC-2 tissue chopper (Ivan Sorvall, Inc., Newtown, Conn).[8] After rinsing in cacodylate buffer to remove fixative, we incubated the sections at 37 C for 2 hours either in a modified Gomori medium, containing 40 mM Tris-maleate buffer, pH 5.0, 2.4 mM lead nitrate, and 11.5 mM β-glycerophosphate (Sigma Chemical Company, St. Louis, Mo) as substrate,[9] or in 20 mM sodium acetate buffer, pH 5.0, 3.6 mM lead nitrate, and 2.7 mM cytidine monophosphate (Sigma Chemical Company) as substrate.[10] Control sections were incubated in medium without substrate. After incubation, the specimens were washed once in cacodylate buffer and postfixed in 1% osmium tetroxide in cacodylate buffer at 0 C. They were then processed for electron-microscopic examination as described above.

Cholesterol

Intracellular location of unesterified cholesterol was identified by the digitonin procedure of Scallen and Dietert.[11] Diced tissue specimens were fixed in Flickinger's aldehyde fixative (2% formaldehyde, 2.5% glutaraldehyde, and 0.05% calcium chloride in 100 mM sodium cacodylate buffer, pH 7.2) for 30 minutes at room temperature. The specimens were then further treated with Flickinger's fixative containing 0.2% digitonin (Fisher Scientific Company, Pittsburgh, Pa) for 1–3 hours at room temperature. The specimens were postfixed in 1% osmium tetroxide in cacodylate buffer, and processed for electron microscopy as described above, except that dehydration (5–10 minutes) in graded solutions (20%, 30%, 50%, 95%, and 100%) of ethyl alcohol was used and the propylene oxide step was omitted. Infiltration with Epon was done in 1 : 1 (vol/vol) mixtures of Epon and alcohol, followed by Epon alone.

Results

Ultrastructure of Tissues of Affected Mice

The intracellular inclusions described here were found in tissues of both male and female affected mice. The structures had the same appearance and frequency in both sexes.

Liver

Sinusoids were obstructed by numerous large foam cells and erythrocytes, resulting in disruption of the usual organization of the tissue (Figure 1A). The foam cells were filled with large vacuolated inclusions; many of these cells were presumably Kupffer cells, but the degree of cytoplasmic vacuolization was so extensive that identification could not be established with certainty. Erythrocytes were sometimes found in the cytoplasm of the foam cells, indicating that these cells were phagocytic.

Hepatocytes exhibited numerous inclusions, some consisting of vacuoles containing osmiophilic bodies and others consisting of rhomboidal crystal clefts (Figure 1B). The inclusions tended to be concentrated near the bile canaliculi, although they could be found

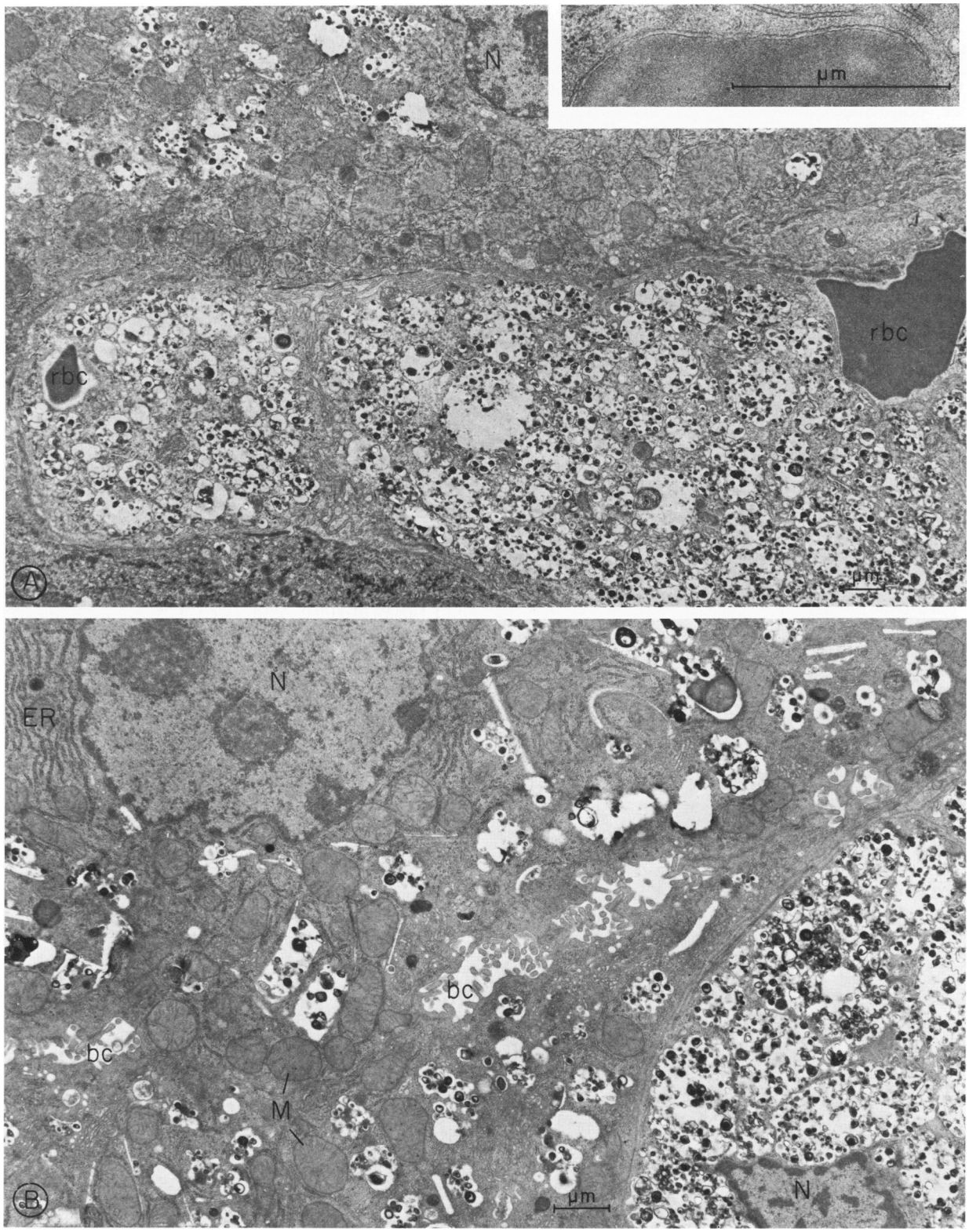

Figure 1 — Appearance of liver parenchyma of an affected NCTR-BALB/c mouse. **A** — Foam cells filled with inclusions obstruct a sinusoid, which extends across the lower half of the micrograph. Nearby hepatocytes also possess inclusions like those in the foam cells. Erythrocytes (*rbc*) are present in the sinusoid, and some are phagocytized by the foam cells, as shown in the inset, in which the phagosome membrane is clearly visible. **B** — Portions of cytoplasm of several hepatocytes with numerous crystal clefts as well as inclusions similar in appearance to those found in adjacent foam cells (*lower right*). Hepatocyte inclusions are generally smaller, and they tend to cluster near bile canaliculi (*bc*). Nucleus (*N*), mitochondrion (*M*), and endoplasmic reticulum (*ER*) appear normal. (**A**, ×7800; **inset**, ×35,000; **B**, ×10,000) (With a photographic reduction of 7%)

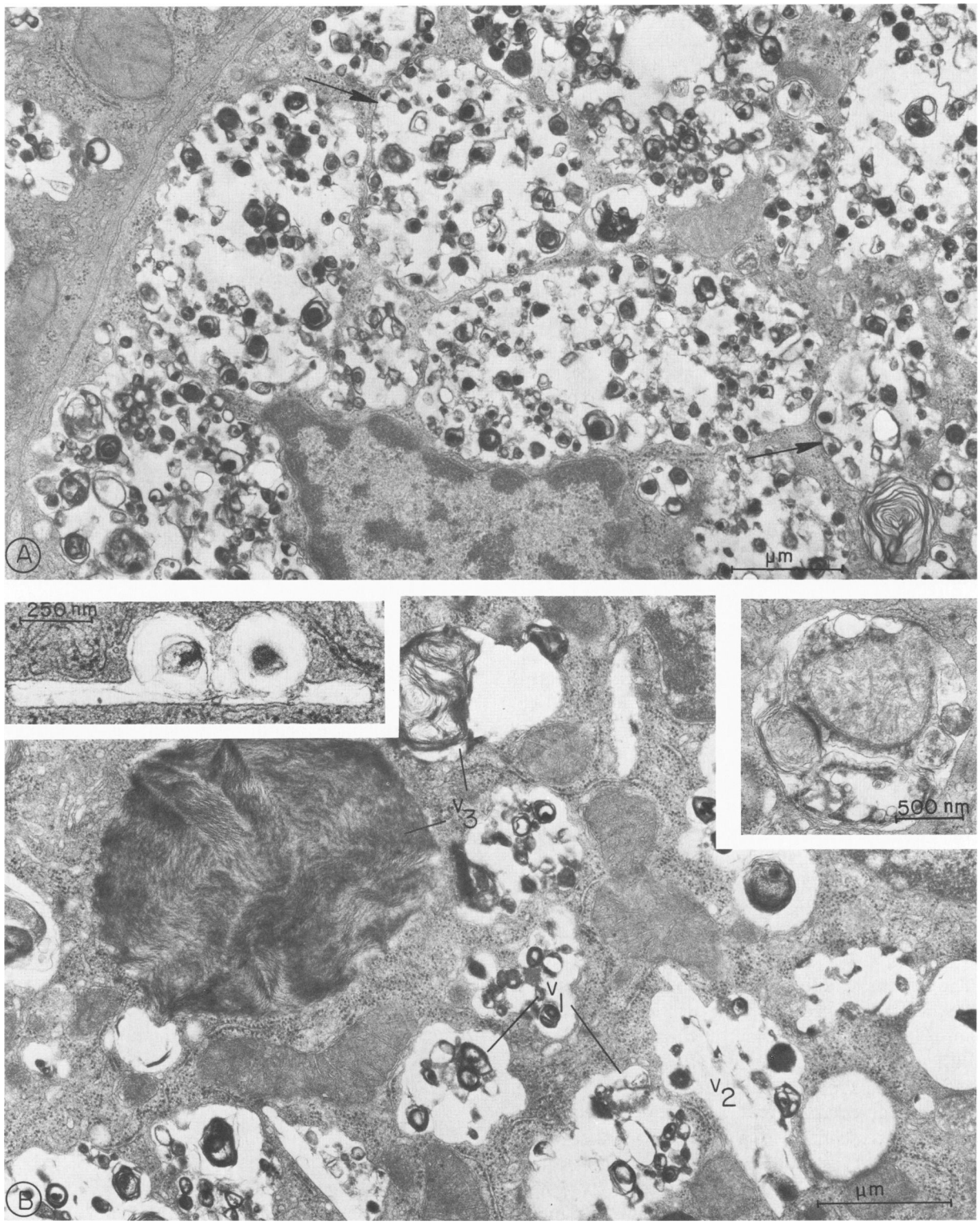

Figure 2—Detailed views of the inclusions in liver. **A**—Inclusions in cytoplasm of sinusoid foam cell are large vacuoles bound by a membrane (*arrows*). They contain numerous lamellated, osmiophilic bodies 100–500 nm in diameter that are interspersed in electron-lucent areas, presumed to represent lipid extracted during tissue processing. **B**—Portion of hepatocyte cytoplasm showing the polymorphic nature of the inclusions. The most frequent vacuoles (v_1) are similar to those seen in foam cells. Crystal clefts may appear in these structures (v_2), better illustrated in upper **left inset**, where limiting membrane is visible. Occasionally, vacuoles filled with membraneous whorls (v_3) or autophagic remnants of mitochondria and endoplasmic reticulum (**right inset**) can be seen. (**A**, ×20,000; **B**, ×24,000; **left inset**, ×54,000; **right inset**, ×25,000) (With a photographic reduction of 7%)

throughout the hepatocyte cytoplasm. In favorable sections, endothelial cells and fat-storing cells were also seen to possess inclusions, but these were fewer in number than in the hepatocytes or the foam cells.

The inclusions present in sinusoidal foam cells and hepatocytes are shown at higher magnification in Figure 2. The foam cell inclusions consisted of vacuoles 2–5 μ in diameter bound by a membrane and containing numerous lamellated bodies ranging from 200 to 500 nm in diameter (Figure 2A). The lamellated bodies often possessed osmiophilic dense centers possibly derived from tightly coiled myelinlike material.

The hepatocyte inclusions were also membrane-bounded but were smaller in size than those found in foam cells and were more variable in appearance (Figure 2B). The most common form of hepatocyte inclusion contained lamellated bodies similar in appearance to those seen in the foam cells. Other inclusions consisted of crystal clefts surrounded by a membrane. Often, crystal clefts, together with lamellated bodies, were seen in the same vacuole. The crystal clefts appeared in both glutaraldehyde and paraformaldehyde–glutaraldehyde fixed tissues. Less commonly observed were vacuoles filled with tightly packed membranous whorls. Autophagic vacuoles were seen more frequently in the hepatocytes of affected NCTR-BALB/c mice than in those of control animals; typical secondary lysosomes were scarce. Lipid droplets and glycogen, abundant in hepatocytes from unaffected mice, were absent. Their absence and the frequent appearance of autophagic vacuoles could be a reflection of the nutritional state of the animals. Other cytoplasmic structures, such as the endoplasmic reticulum, Golgi apparatus, mitochondria, and peroxisomes, appeared normal in the liver cells of affected animals.

Spleen

The spleens of affected mice showed lipid deposits in the cells of the red pulp and marginal zone. Giant foam cells as large as 30 μm in diameter were seen, and they contained large inclusions similar in appearance to those found in foam cells in liver (Figure 3A). Again, the inclusions were membrane-bounded and in some instances contained crystal clefts. Most of the foam cells were presumably derived from free or fixed macrophages. Lymphocytes in the white pulp were also affected, but not to the severe degree found in the foam cells of the red pulp. The lymphocyte inclusions were similar to those in the foam cells but were fewer and smaller (Figure 3B). Other cells found in the spleen, such as smooth muscle cells and reticular cells, contained occasional small inclusions. The blood leukocytes were also altered (not shown).

Lung

Alveolar macrophages were the cells most affected in the lung (Figure 3C). They were enlarged and possessed inclusions similar to those seen in foam cells of liver and spleen. Pneumocytes, on the other hand, rarely contained the inclusions.

Other Tissues

The inclusions described above were seen also in cells of several other tissues of affected mice (not illustrated). Depending on the source of the tissue, the internal appearance of inclusions varied slightly. Sometimes amorphous materials or loosely coiled myelinlike figures were present. Small cytoplasmic inclusions were seen in tubular epithelium of the kidney and in neuroglial cells of the brain. Epithelial cells and goblet cells in the intestinal villi did not exhibit the inclusions, but cells in the lacteals were affected. As in spleen, the lymph nodes possessed numerous foam cells filled with large inclusions, and the cytoplasm of lymphocytes in germinal centers often contained clusters of small inclusions.

Cytochemical Studies

Acid Phosphatase

As shown in Figure 4, cytochemical reaction for acid phosphatase identified the inclusions of both liver sinusoid foam cells and hepatocytes as lysosomes. The staining was observed in these structures with either β-glycerophosphate or cytidine monophosphate as substrates. Lead phosphate reaction product did not appear in the inclusions in the absence of substrate. Some inclusions did not stain, particularly those in the sinusoid foam cells. This could reflect the lack of enzyme activity but could also be the consequence of enzyme inactivation due to fixation or, since the inclusions are so large in foam cells, it could be accounted for by formation of the reaction product above or below the plane of section. The lysosome contents themselves might also inhibit enzyme activity.

Cholesterol

Digitonin treatment of liver tissue of affected mice resulted in the appearance of tubular structures (Figure 5). These occurred throughout the cytoplasm of the foam cells and in discrete circumscribed sites in the hepatocytes. These structures, called spicules, are characteristic of digitonide complexes of cholesterol[11–13] and phospholipid.[14] Typical storage inclusions were absent after digitonin treatment. Remnants of lamellated bodies, however, were sometimes found

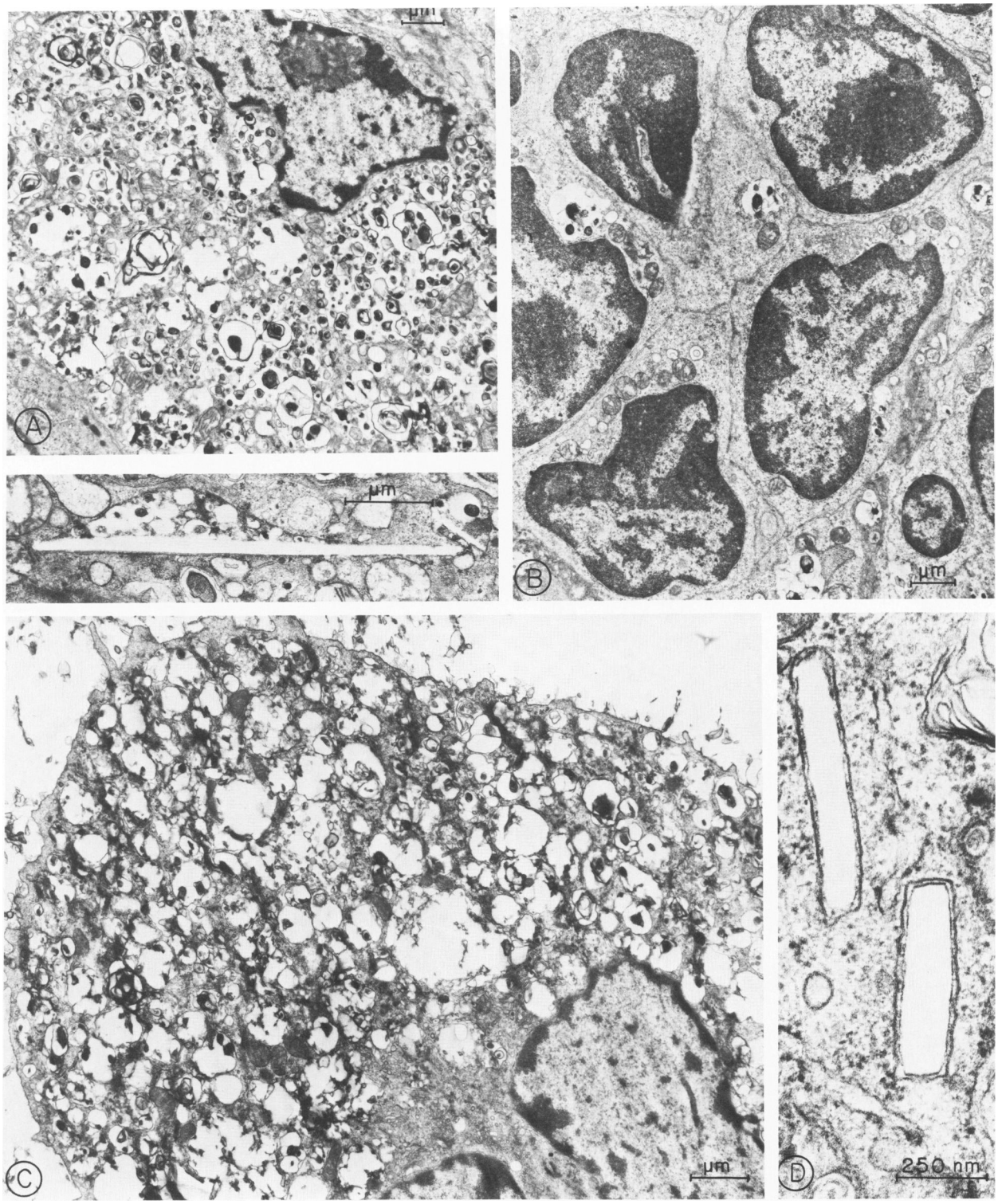

Figure 3 — Appearance of other tissues of an affected NCTR-BALB/c mouse. **A** — Foam cell in splenic red pulp is filled with vacuolar inclusions delimited by a membrane; crystals may form in the vacuole (**inset**). **B** — Lymphocytes in splenic white pulp are less affected. The vacuolar inclusions are smaller and fewer in number. **C** — Typical foam cell free in the alveolar space of lung. **D** — Example of a membrane-limited crystal cleft in cytoplasm of alveolar foam cell cytoplasm. (**A**, ×7800; **inset**, ×15,000; **B**, ×7800; **C**, ×9800; **D**, ×62,000) (With a photographic reduction of 5%)

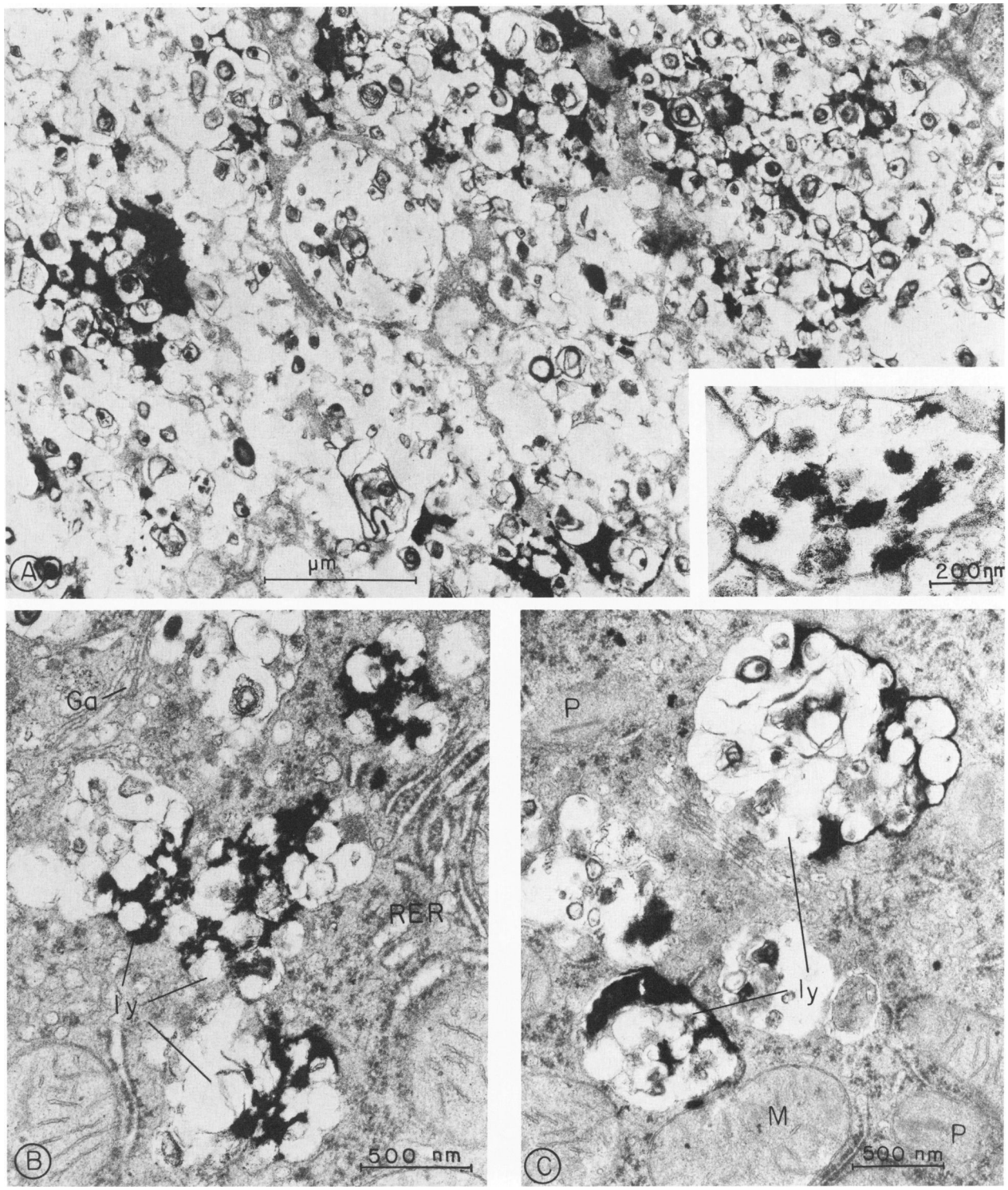

Figure 4 — Cytochemical demonstration of liver inclusions as lysosomes. **A** — Acid phosphatase reaction product associated with inclusions in cytoplasm of a liver foam cell. **Inset** — Reaction product in a membrane delimited vacuole. **B** and **C** — Two views of hepatocyte cytoplasm showing several inclusions (*ly*) that possess acid phosphatase. *Ga*, Golgi apparatus; *M*, mitochondrion; *RER*, rough endoplasmic reticulum; *P*, peroxisome. (**A**, ×27,000; **inset**, ×55,500; **B**, ×39,000; **C**, ×32,000) (With a photographic reduction of 6%)

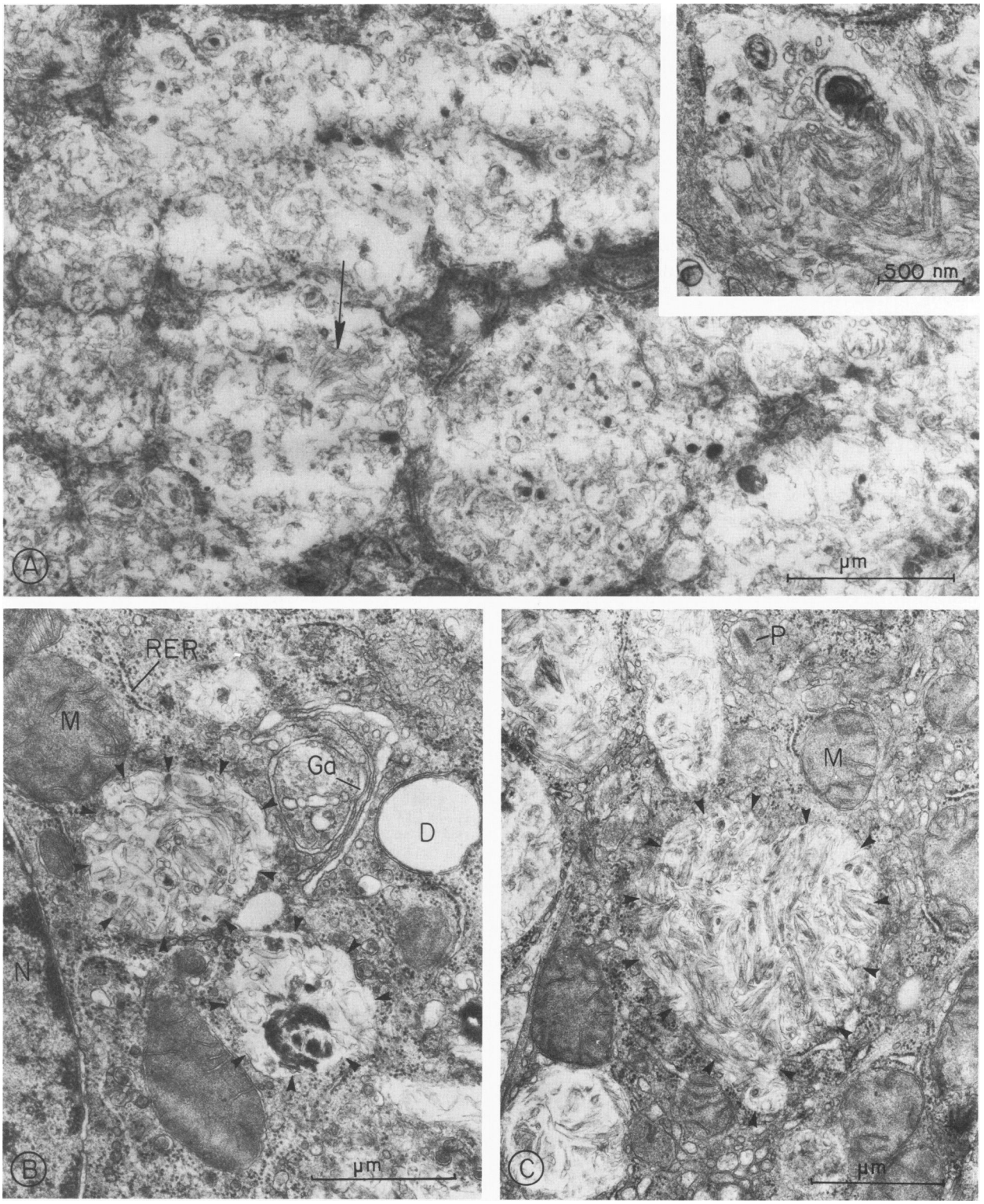

Figure 5 — Appearance of liver inclusions after digitonin treatment. **A** — The vacuolar contents of foam cell cytoplasm are replaced by tubular digitonide "spicules" (*arrow*). The delimiting membrane of the vacuoles are no longer evident. **Inset** — A detailed view of an inclusion filled with spicules; a lamellated osmiophilic body is seen among the spicules. **B** and **C** — Two views of hepatocyte cytoplasm illustrating spicules in discrete areas (*arrowheads*). Note in **B** the small cytoplasmic lipid droplet (*D*) not altered by the digitonin treatment. Other cellular components such as nucleus (*N*), mitochondrion (*M*), rough endoplasmic reticulum (*RER*), Golgi apparatus (*Ga*), and peroxisome (*P*) appear unaffected by the digitonin. (**A**, ×25,000; **inset**, ×32,000; **B**, ×27,000; **C**, ×24,000) (With a photographic reduction of 6%)

among clusters of spicules, indicating that the digitonin reacted with the contents of inclusions to alter the appearance of the vacuoles. Other cellular organelles, including endoplasmic reticulum, mitochondria, and peroxisomes, did not exhibit spicules and appeared unchanged.

Discussion

We conclude from the morphologic observations presented above that the intracellular inclusions appearing in tissues of affected NCTR-BALB/c mice are lipid-filled lysosomes and that the symptoms of the affected mice are the result of a lysosome storage syndrome. Cholesterol is a major storage product in the lysosomes, as demonstrated by the cytochemical reaction with digitonin and the appearance of cholesterollike crystals in the inclusions. The cholesterol crystals were strikingly more numerous in hepatocytes than in adjacent sinusoid foam cells; we have no explanation for the preferential formation of crystals in the hepatocytes. Very similar intralysosomal cholesterollike crystals and digitonin-induced spicule formation in lysosomes have been described previously in aortic foam cells of rabbits fed on cholesterol-rich diets.[15] The lamellated bodies within the inclusions of NCTR-BALB/c mice may represent phospholipid. Their loosely coiled appearance is comparable to the multilayered structures that are seen in lysosomes of rats with drug-induced phospholipidoses.[16]

Niemann–Pick disease in humans is characterized by tissue accumulations of sphingomyelin and, to a lesser degree, unesterified cholesterol[17] and by the occurrence of large, membrane-bounded cytoplasmic inclusions whose internal structure varies somewhat, depending on the tissue examined.[18–23] The foam cells in brain tissue, bone marrow, and lymph nodes of these patients contain large bodies packed with myelin figures consisting of concentric osmiophilic layers with a periodicity of about 5 nm. Inclusions in liver cells were found to be more electron-translucent but contained membranelike structures.[21–22] The Niemann–Pick inclusions have been identified as lysosomes by acid phosphatase staining.[20] The myelin-filled structures (v_3) shown in Figure 3B are similar to some of the Niemann–Pick inclusions. But they are seen infrequently and could as well be autophagic vacuoles resulting from the semi-fasted state of the affected mice. The majority of the lysosomes found in the affected NCTR-BALB/c mouse tissues are distinctly different from the Niemann–Pick inclusions. They are more electron-lucent and contain clusters of small lamellated bodies, rather than large membranous whorls. We have not found in the literature any reports of cholesterol crystals in the inclusions of Niemann–Pick cells.

We have also compared morphologically the storage inclusions in affected NCTR-BALB/c mice with intracellular inclusions in tissues of mice with foam cell reticulosis (fm/fm).[24] Tissue accumulations of cholesterol and sphingomyelin also occur in selected tissues of the latter. The two types of inclusions resemble each other only in being membrane-bounded. Their internal structures are dissimilar. In liver, for example, the hepatocyte inclusions of the fm/fm mouse contained an electron-dense matrix in which one or more electron-lucent areas were found; other hepatocyte inclusions were described as tubular in shape. Splenic macrophage inclusions in the fm/fm mice contained a granular matrix with no lamellated bodies. Proliferation of smooth endoplasmic reticulum, which was prominent in hepatocyte cytoplasm of the fm/fm mice, does not occur in liver cells of affected NCTR-BALB/c mice.

References

1. Morris MD, Bhuvaneswaran C, Shio H, Fowler S: Lysosome lipid storage disorder in NCTR-BALB/c mice: I. Description of the disease and genetics. Am J Pathol 1982, 108:140–149
2. Hers HG, Van Hoof F, editors: Lysosomes and Storage Diseases. New York, Academic Press, 1973
3. Shio H, Fowler S, Bhuvaneswaran C, Morris M: Lipid storage syndrome in NCTR-BALB/c mice: Cytochemical and biochemical evidence for accumulation of cholesterol in lysosomes (Abstr). Fed Proc 1981, 40:349
4. Karnovsky MJ: The ultrastructural basis of capillary permeability studied with peroxidase as tracer. J Cell Biol 1967, 35:213–236
5. Farquhar MG, Palade GE: Cell junctions in amphibian skin. J Cell Biol 1965, 26:263–291
6. Watson ML: Staining of tissue sections for electron microscopy with heavy metals. J Biophys Biochem Cytol 1958, 4:475–478
7. Reynolds ES: The use of lead citrate at high pH as an electron-opaque stain in electron microscopy. J Cell Biol 1963, 17:208–213
8. Smith RE, Farquhar MG: Preparation of non-frozen sections for electron microscope cytochemistry. RCA Sci Inst News 1965, 10:13–18
9. Barka T, Anderson PJ: Histochemical methods for acid phosphatase using hexazonium pararosanilin as coupler. J Histochem Cytochem 1962, 10:741–753
10. Novikoff PM, Novikoff AB, Quintana N, Hauw J-J: Golgi apparatus, GERL, and lysosomes of neurons in rat dorsal root ganglia studied by thick section and thin section cytochemistry. J Cell Biol 1971, 50:859–886
11. Scallen TJ, Dietert SE: The quantitative retention of cholesterol in mouse liver prepared for electron microscopy by fixation in a digitonin-containing aldehyde solution. J Cell Biol 1969, 40:802–813
12. Ökrös I: Digitonin reaction in electron microscopy. Histochemie 1968, 13:91–96

13. Williamson JR: Ultrastructural localization and distribution of free cholesterol (3 β-hydroxysterols) in tissues. J Ultrastruct Res 1969, 27:118–133
14. Frühling J, Penasse W, Sand G, Claude A: Reactions de la digitonine avec le cholesterol et autres lipides de la corticosurrénale du rat: Etude par éléctron microscopie. J Microsc (Paris) 1971, 12:83–106
15. Shio H, Haley NJ, Fowler S: Characterization of lipid-laden aortic cells from cholesterol-fed rabbits: III. Intracellular localization of cholesterol and cholesteryl ester. Lab Invest 1979, 41:160–167
16. Lüllmann-Rauch R: Drug-induced lysosomal storage disorders, Lysosomes in Applied Biology and Therapeutics. Edited by JT Dingle, PJ Jacques, IH Shaw. Amsterdam, New York, North-Holland Publishing Co., 1979, pp 49–130
17. Fredrickson DS, Sloan HR: Sphingomyelin lipidoses: Niemann-Pick disease, The Metabolic Basis of Inherited Diseases. 3rd edition. Edited by JB Stanbury, JB Wyngaarden, DS Fredrickson. New York, McGraw-Hill, 1972, pp 783–807
18. Lynn R, Terry RD: Lipid histochemistry and electron microscopy in adult Niemann-Pick disease. Am J Med 1964, 37:987–994
19. Wallace BJ, Schneck L, Kaplan H, Volk BW: Fine structure of the cerebellum of children with lipidoses. Arch Pathol 1965, 80:466–486
20. Lazarus SS, Vethamany VG, Schneck L, Volk BW: Fine structure and histochemistry of peripheral blood cells in Niemann-Pick disease. Lab Invest 1965, 17: 155–170
21. Volk BW, Wallace BJ: The liver in lipidosis: An electron microscopic and histochemical study. Am J Pathol 1966, 49:203–225
22. Wallace BJ, Lazarus SS, Volk BW: Electron microscopic and histochemical studies of viscera in lipidoses, Inborn Disorders of Sphingolipid Metabolism. Edited by SM Aronson, BW Volk. Oxford Pergamon Press, 1967, pp 107–120
23. Vethamany VG, Welch JP, Vethamany SK: Type D Niemann-Pick disease (Nova Scotia variant). Arch Pathol 1972, 93:537–543
24. Adachi M, Tsai C-Y, Hoffman LM, Schneck L, Volk BW: The central nervous system, liver, and spleen of FM mice. Arch Pathol 1974, 97:232–238